Applied Energy 114 (2014) 417–425

Contents lists available at ScienceDirect

Applied Energy

journal homepage: www.elsevier.com/locate/apenergy

Simulation and exergetic evaluation of CO_2 capture in a solid-oxide fuel-cell combined-cycle power plant

Fontina Petrakopoulou [a,b,*], Young Duk Lee [c,d], George Tsatsaronis [c]

[a] National Technical University of Athens, Iroon Polytechneiou 9, 15773 Athens, Greece
[b] Technical University of Crete, University Campus, 73100 Chania, Greece
[c] Technische Universität Berlin, Marchstr. 18, 10587 Berlin, Germany
[d] Korea Institute of Machinery & Materials, 171 Jang-dong, Yusoneg-gu, Daejeon 305-343, South Korea

HIGHLIGHTS

- An exergetic analysis is used to identify the thermodynamic irreversibilities of a power plant.
- The plant includes a solid-oxide fuel-cell unit and CO_2 capture.
- Additional power generated in the fuel-cell unit enhances the power output of the plant.
- The power plant results in a high efficiency compared both to conventional and other CO_2 capture plants.
- High irreversibilities are found for the solid-oxide fuel cell.

ARTICLE INFO

Article history:
Received 11 September 2012
Received in revised form 19 August 2013
Accepted 17 September 2013

Keywords:
SOFC
Fuel cell
CO_2 capture
Exergetic analysis
Combined-cycle power plant

ABSTRACT

The incorporation of fuel cells into power plants can enhance the operational efficiency and facilitate the separation and capture of emissions. In this paper a fuel-cell unit, consisting of solid-oxide fuel-cell stacks, a pre-reformer, and an afterburner is incorporated into a combined-cycle power plant with CO_2 capture. The thermodynamic performance of the plant is examined using an exergetic analysis and it is compared with a conventional combined-cycle power plant (reference plant) without CO_2 capture, as well as with other plants with CO_2 capture.

The inefficiencies of the chemical reactions taking place in the fuel-cell unit are found to be the main source of exergy destruction among the plant components. However, the additional power generated in the fuel-cell stacks and the afterburner enhances the overall efficiency and compensates for the energy needed for the capture and compression of the carbon dioxide. When compared with the reference plant and with alternative capture technologies, the solid-oxide fuel-cell plant with CO_2 capture operates more efficiently and appears to be a thermodynamically promising approach for carbon capture.

1. Introduction

Solid-oxide fuel cells (SOFCs) are regarded as one of the most promising technologies in the power-generation industry for their high efficiency, high operating temperature, and low emissions that allow various applications for heat and power generation [1,2].

Harvey and Richter [3] first proposed the combination of a Brayton cycle with fuel cells, forming the basis of various studies evaluating different incorporation possibilities of SOFCs into gas turbines systems (e.g., [4–6]). Siemens Energy reported to have successfully demonstrated the concept with a 220 kW unit at the University of California and a 300 kW unit in Pittsburgh. Moreover, Mitsubishi Heavy Industries (MHI) reported to have developed a 200 kW-class SOFC-GT hybrid system combining a tubular type SOFC stack with an internally developed gas turbine. The system was reported to operate successfully with a net electrical efficiency of 52% [7].

The operation of a hybrid SOFC-GT system in partial load conditions was investigated by Calise et al. [8]. In 2003, Onda et al. studied the effcts of different parameters of an SOFC when incorporated into a steam injected gas turbine (STIG) cycle and reported a possible efficiency improvement of 1–3% [9]. In the same year the integration of a humid air turbine (HAT) into an SOFC system was simulated and studied [6,10]. Panopoulos et al. [11] and El-Emam et al. [12] studied the operation of an SOFC in a power plant with coal gasification and a combined heat and power plant (CHP) with biomass gasification, respectively. Akkaya et al. [13] investigated efficiency improvements of an SOFC/GT cogeneration system and Zink et al. [14] researched an SOFC absorption

* Corresponding author at: National Technical University of Athens, Iroon Polytechneiou 9, 15773 Athens, Greece. Tel.: +30 2107722334; fax: +30 2107723285.
E-mail address: f.petrakopoulou@chemeng.ntua.gr (F. Petrakopoulou).

0306-2619/$ - see front matter © 2013 Elsevier Ltd. All rights reserved.
http://dx.doi.org/10.1016/j.apenergy.2013.09.034

Nomenclature

$\dot{E}$	exergy rate (MW)
p	pressure (bar)
T	temperature (°C)
$\dot{W}$	power input/output (MW)
y	exergy destruction ratio (%)

Subscripts

D	exergy destruction
F	fuel (exergy)
gen	power generation
P	product (exergy)
in	input
k	component
L	loss
tot	overall system

Abbreviations

AFB	afterburner
APH	air preheater
C1-C5	compressors
COND	condenser
COOL	cooler
CT	cooling tower
EC	economizer
EV	evaporator
FG	flue gas
GEN	generator
GT	gas turbine
HP	high pressure
HT	high temperature
HRSG	heat-recovery steam generator
IP	intermediate pressure
LP	low pressure
LT	low temperature
NG	natural gas
P	pump
PH	preheater
PR	pre-reformer
SH	superheater
SOFC	solid-oxide fuel-cell
ST	steam turbine

Greek letter

ε	exergetic efficiency

heating and cooling system, finding both technical and environmental advantages of such a coupling. Gadalla and Al Aid [15] reported an efficiency improvement of 5% when combining an SOFC with a PEMFC (polymer electrolyte membrane fuel cell) in a GT system. A trigeneration plant combining an SOFC with an organic Rankine cycle (ORC) was studied by Al-Sulaiman et al. [16] showing relatively promising results. Lastly, Rajashekara [17] studied the operation of various hybrid plants with fuel cells, including the coupling of an SOFC with a thermo-photovoltaic power generation unit.

Although various studies on SOFC applications and integration exist, large-scale SOFCs are not yet commercially available and the technology cannot be considered fully developed. Additionally, fuel-cell technology is associated with high costs and various technical problems, such as fuel gas desulfurization, reforming and short stack working life. Nevertheless, the relatively high efficiencies and the lower emissions achieved with fuel cells make them attractive from an environmental viewpoint [18]. Overall, when compared to other alternatives, combining hybrid GT/SOFC systems with CO_2 capture is an option to achieve very low emissions with relatively high efficiency [19].

Carbon capture and storage (CCS) is suggested as a means for mitigating climate change linked to the combustion of fossil fuels [20,21]. Thus, it is important to evaluate the feasibility of alternative CCS technologies [22–25]. CO_2 capture can be separated into three main groups: post-combustion, pre-combustion and oxy-fuel combustion, depending on the oxidant used in the combustion, and on whether the capture is realized before or after the combustion.

In this paper, we present an oxy-fuel, large-scale combined-cycle power plant, in which the combustion chamber is replaced by an integrated pressurized SOFC unit [26–28]. The plant includes CO_2 separation and compression and its structure is based on a conventional reference combined-cycle power plant without emission reduction [29–31]. The thermodynamic performance of the CO_2 capture plant is examined using an exergetic analysis, with which irreversibilities within components and component efficiencies are calculated. The operation of the plant is compared to that of the conventional reference plant, as well as to other CO_2 capture technologies [32]. Finally, important strategies that would improve the overall plant performance are discussed.

2. Methodology

2.1. Principles of an exergetic analysis

Exergy is the maximum theoretical work obtainable from a thermal system, as the system is brought into thermodynamic equilibrium with the environment, while interacting with this environment only [33]. Neglecting nuclear, magnetic, electrical and surface tension effects, the total exergy of a system, $\dot{E}_{sys}$, consists of four parts: physical, kinetic, potential and chemical exergy:

$$\dot{E}_{sys} = \dot{E}^{PH} + \dot{E}^{KN} + \dot{E}^{PT} + \dot{E}^{CH} \quad (1)$$

Here, the kinetic and potential exergy are neglected because the system is considered to be at rest, relative to the environment. The specific physical exergy of a material stream is obtained from:

$$e^{PH} = (h - h_0) - T_0(s - s_0) \quad (2)$$

where h_0 and s_0 are the specific enthalpy and entropy, respectively, of the stream being considered at the reference state, and h and s are the specific enthalpy and entropy at the given thermodynamic state. The chemical exergy per mole of gas of a mixture of n gases is calculated with Eq. (3), where e_i^{CH} and x_i are the standard molar chemical exergy and the mole fraction of each substance i, respectively.

$$e^{CH} = \sum_{i=1}^{i=n} x_i e_i^{CH} + RT_0 \sum_{i=1}^{i=n} \ln(x_i) \quad (3)$$

The total exergy rate of stream j is calculated by multiplying its total specific exergy, $e_j = e^{PH} + e^{CH}$ with its mass flow rate, $\dot{m}_j$:

$$\dot{E}_j = \dot{m}_j e_j \quad (4)$$

In an exergetic analysis of an energy conversion system, the exergy of the fuel and exergy of the product must be defined at the component level of the plant. To realize this, the principles presented by Tsatsaronis and Cziesla have been adopted [34]. The ratio between the exergy of the product and fuel of a component constitutes its exergetic efficiency:

$$\varepsilon_k = \frac{\dot{E}_{P,k}}{\dot{E}_{F,k}} \tag{5}$$

Thermodynamic processes are governed by mass and energy conservation laws. Exergy is not conserved and it can be destroyed due to inefficiencies. The exergy destruction $\dot{E}_D$ is mainly associated with chemical reactions, heat exchange, fluid friction, and the mixing of streams at different states. The rate of exergy destruction within component k is given by:

$$\dot{E}_{D,k} = \dot{E}_{F,k} - \dot{E}_{P,k} \tag{6}$$

The ratio of the exergy destruction within component k and the exergy of the fuel provided to the overall plant, $\dot{E}_{F,tot}$, constitutes the component's exergy destruction ratio:

$$y_{D,k} = \frac{\dot{E}_{D,k}}{\dot{E}_{F,tot}} \tag{7}$$

The exergetic efficiency of the overall thermodynamic system is calculated as:

$$\varepsilon_{tot} = \frac{\dot{E}_{P,tot}}{\dot{E}_{F,tot}} = 1 - \frac{\dot{E}_{D,tot} + \dot{E}_{L,tot}}{\dot{E}_{F,tot}} \tag{8}$$

Here, $\dot{E}_{L,tot}$ represents the exergy loss of the plant, i.e., the thermodynamic inefficiencies associated with exergy streams exiting the system, and $\dot{E}_{D,tot}$ is the exergy destruction within the overall plant.

3. The SOFC plant

The main assumptions applied to the simulation of the plant are presented in Table 1, while a more detailed description of the operation of the components constituting the SOFC unit is provided below. The software EbsilonProfessional was used for the simulation of the thermodynamic system [35].

3.1. Assumptions for modeling the SOFC unit

The SOFC unit consists of a pre-reformer (PR), solid-oxide fuel-cell stacks and an afterburner (AFB), which have been simulated with the appropriate embedded chemical reactions, mass and energy balances and reaction conditions. The PR is used to convert the methane into a gas rich in hydrogen, CO and CO_2. In this way, damage that would have been caused to the cell by soot formation during the direct reforming of the methane is avoided. The data used for the SOFC unit in the considered plant were based on the study presented in [26].

Table 1
Simulation assumptions.

Fuel (CH_4)	50.1 MJ/kg, 14 kg/s, 50 bar, 15 °C
Air	1.01 bar, 15 °C
SOFC operating conditions	1000 °C, 9.03 bar, 0.70 V
Afterburner (AFB) operating conditions	1000 °C, 8.57 bar, 0.30 V
Fuel utilization ratio, SOFC (%)	85
Fuel utilization ratio, AFB (%)	95
Steam/carbon ratio (−)	2
Air/fuel ratio (−)	24.13
Pressure losses in reactors (%)	5

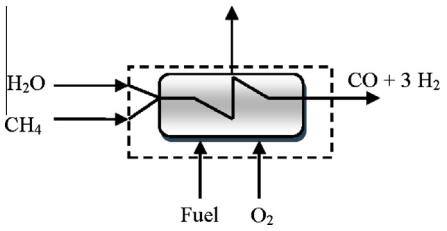

Fig. 1. Schematic of a steam reformer.

Reformer-fuel-cell systems are still under investigation, but natural gas steam reforming is a common process. A simplified schematic of a steam reformer, where water vapor and methane react under high temperature to produce H_2 and CO, is shown in Fig. 1. Fig. 2 presents the overall power plant simulated with the incorporated SOFC and CO_2 capture and compression units.

The external PR assumed here includes a strongly endothermic reforming reaction and the slightly exothermic water gas shift reaction (Eqs. 9 and 10). We assume that both reactions are adiabatic and take place at chemical equilibrium.

$$CH_4 + H_2O \Longleftrightarrow CO + 3H_2 \tag{9}$$

$$CO + H_2O \Longleftrightarrow CO_2 + H_2 \tag{10}$$

The necessary water for the reactions is provided by recycling part of the gas exiting the anode of the SOFC to the inlet of the PR (Stream 85, Fig. 2). The component used to compensate for the pressure drop within the PR and SOFC is a hot gas fan driven with power generated in an additional steam turbine (ST4) [36]. The recirculation ratio is determined by the steam/carbon ratio, which was set to 2. The temperature of Stream 60 (preheated methane) is calculated using the mass and energy balances of the PR.

The reforming of unconverted hydrocarbons, the shift reaction and the electro-chemical reaction take place in the SOFC stacks (Eqs. 9-11), assuming that only hydrogen reacts electrochemically with the oxygen ions.

$$H_2 + O^{2-} \Longleftrightarrow H_2O + 2e^- \tag{11}$$

In order to maintain the energy balance of the SOFC stacks, the net heat released by Reactions (9) and (10) must be equal to the heat consumed to increase the temperature of the incoming streams of the anode and cathode (Streams 83 and 93) to the operating temperature. With these assumptions, the temperature of the incoming air (Stream 93) is calculated. The operating voltage, temperature, pressure and fuel utilization in the stacks have been assumed to be 0.70 V, 1000 °C, 9.03 bar and 85%, respectively. Because the voltage (0.70 V) is rather low for power supply, we assume several cells in stacks to increase the overall voltage of the fuel cell.

To determine the power output of the fuel cells, the electric current must be determined first. If the converted moles of hydrogen are n_{H_2}, the electrons and oxygen ions are $2n_{H_2}$ (Reaction 11). The electric current, I_{SOFC}, and the power output, $\dot{W}_{shaft}$, are then calculated as:

$$I_{SOFC} = 2n_{H_2} \times F \tag{12}$$

$$\dot{W}_{SOFC} = I_{SOFC} \times V \times 0.95 \tag{13}$$

where, F is the Faraday constant (F = 96,487 C/mol) and V is the operating voltage [2]. The loss associated with the DC/AC conversion has been assumed to be 5%.

The afterburner, AFB, was simulated as an SOFC-afterburner leading to additional electricity production [27]. However, here, the operating voltage is too low to achieve high fuel utilization

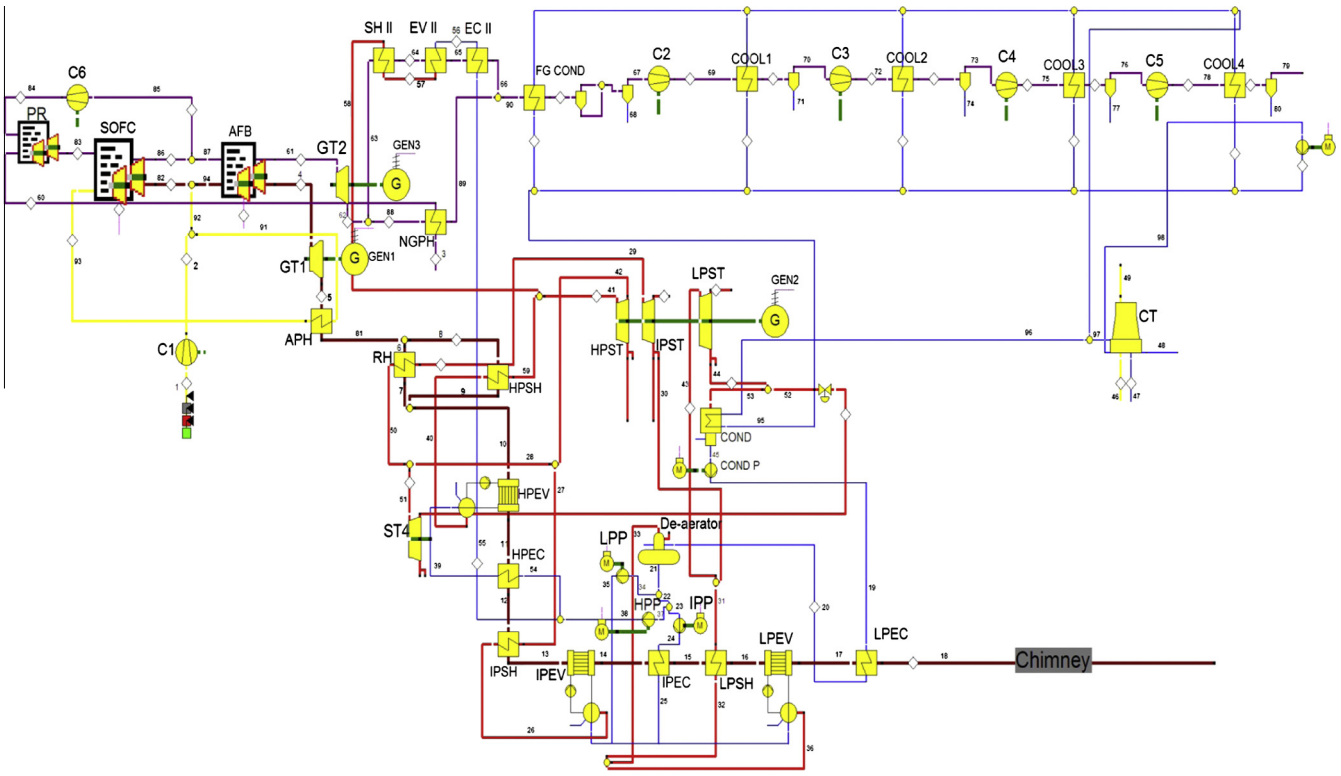

Fig. 2. The structure of the SOFC plant.

Table 2
Incoming and outgoing exergy streams.

	$\dot{E}_j$ (MW)	(%)
Incoming exergy streams	852.6	100.00
$\dot{E}_{NG}$	729.6	85.58
$\dot{E}_{Air}$	0.5	0.06
$\dot{E}_{W_{C1}}$	101.1	11.86
$\dot{E}_{W_{C6/Fan}}$	4.9	0.57
$\dot{E}_{W_{C2-C5}}$	15.9	1.87
$\dot{E}_{W_{Pumps}}$	0.5	0.06
Outgoing and product exergy streams		
$\dot{E}_{W,SOFC}$	381.1	44.70
$\dot{E}_{W,AFB}$	27.6	3.24
$\dot{E}_{W_{GT1,GT2,Brutto}}$	190.4	22.33
$\dot{E}_{W_{STs,Brutto}}$	42.2	4.95
$\dot{E}_{loss,water}$	0.1	0.01
$\dot{E}_{loss,exhaust}$	4.8	0.56
$\dot{E}_{CO_2}$	28.8	3.38
$\dot{E}_{D,tot}$	177.6	20.83

Table 3
Definitions of the exergy of fuel and product for selected components of the SOFC plant.

Plant components	Exergy of the product, $\dot{E}_P$	Exergy of the fuel, $\dot{E}_F$
C1	$\dot{E}_2 - \dot{E}_1$	$\dot{E}_{W_{C1}}$
SOFC	$\dot{E}_{W,SOFC} + \dot{E}^{PH}_{86} + \dot{E}^{PH}_{82} - \dot{E}^{PH}_{83} - \dot{E}^{PH}_{93}$	$\dot{E}^{CH}_{83} + \dot{E}^{CH}_{93} - \dot{E}^{CH}_{86} - \dot{E}^{CH}_{82}$
PR	$\dot{E}^{CH}_{83} - \dot{E}^{CH}_{84} - \dot{E}^{CH}_{60}$	$\dot{E}^{PH}_{84} + \dot{E}^{PH}_{60} - \dot{E}^{PH}_{83}$
AFB	$\dot{E}_{W,AFB} - \dot{E}^{PH}_{87} - \dot{E}^{PH}_{94} + \dot{E}^{PH}_{4} + \dot{E}^{PH}_{61}$	$\dot{E}^{CH}_{87} + \dot{E}^{CH}_{94} - \dot{E}^{CH}_{4} - \dot{E}^{CH}_{61}$
GT1	$\dot{E}_{W_{GT1}}$	$\dot{E}_4 - \dot{E}_5$
APH	$\dot{E}_{93} - \dot{E}_{91}$	$\dot{E}_5 - \dot{E}_{81}$
HPST	$\dot{E}_{W_{HPST}}$	$\dot{E}_{41} - \dot{E}_{42}$

with a relatively small cell area [18]. The electrolyte of the SOFC acts as a highly selective membrane for the transport of oxygen ions from the cathode to the anode. Since 85% of the CH_4 is converted to H_2 and CO in the SOFC stacks, only carbon monoxide and hydrogen oxidation take place in the AFB. The fuel utilization in the AFB for current SOFC technology using Ni-cermet anodes is lower than 95% at 1000 °C, due to NiO formation. This results in approximately complete fuel utilization: 99.25% (with 85% converted in the fuel cell and 95% in the AFB: 0.85+(1-0.85)x0.95) [27]. Thus, the SOFC can act as an "afterburner" and approach complete oxidization of the fuel without introducing nitrogen. This concept has been proposed as a demonstration project funded mainly by A/S Norske Shell [28].

The operating voltage, temperature and pressure of the AFB in this work were set to 0.30 V, 1000 °C and 8.57 bar, respectively. The assumed loss associated with the DC/AC conversion of the AFB was also 5%.

The simulation of the power plant requires the incorporation of the SOFC unit into a reference power plant (Fig. 2). The reference power plant is a combined-cycle power plant and its thermodynamic evaluation has been presented in [31]. The reference plant does not include CO_2 capture and is used for comparison of the SOFC plant with conventional structures. To perform this comparison under similar conditions and to also compare the SOFC plant with other options for CO_2 capture, all plants are provided with the same amount of fuel and, whenever possible, their operational conditions are kept constant [29].

3.2. Description of the power plant

As seen in Fig. 2, the natural gas entering the SOFC plant (Stream 3) is preheated and fed into the PR, where it reacts with steam (Stream 84, 56% v/v H_2O) to produce H_2 and CO. Air (Stream 1) is compressed to 9.5 bar and is split into two parts (Streams 91

Table A.1
Stream properties of the SOFC power plant.

Stream (j)	m_j (kg/s)	T_j (°C)	p_j (bar)	$\dot{E}_j^{PH}$ (MW)	$\dot{E}_j^{CH}$ (MW)	$\dot{E}_j^{tot}$ (MW)
1	337.81	15.00	1.01	0.00	0.53	0.53
2	337.81	303.85	9.50	93.71	0.53	94.24
3	14.00	15.00	50.00	8.15	721.47	729.62
4	282.26	1000.00	8.57	228.52	1.97	230.49
5	282.26	543.18	1.06	70.23	1.97	72.19
6	122.26	458.29	1.06	23.17	0.85	24.02
7	122.26	441.57	1.05	21.77	0.85	22.62
8	160.00	458.29	1.06	30.32	1.11	31.43
9	160.00	400.17	1.05	24.27	1.11	25.38
10	282.26	418.15	1.05	45.99	1.97	47.96
11	282.26	341.18	1.05	32.75	1.97	34.72
12	282.26	282.03	1.04	23.61	1.97	25.58
13	282.26	279.09	1.04	23.19	1.97	25.16
14	282.26	232.62	1.04	16.84	1.97	18.81
15	282.26	224.25	1.04	15.78	1.97	17.74
16	282.26	220.59	1.04	15.32	1.97	17.28
17	282.26	156.37	1.03	8.13	1.97	10.10
18	282.26	90.90	1.03	2.83	1.97	4.80
19	43.91	32.89	3.73	0.11	0.11	0.22
20	43.91	136.37	3.62	3.73	0.11	3.84
21	44.23	140.01	3.62	3.97	0.11	4.08
22	35.45	140.01	3.62	3.18	0.09	3.27
23	7.38	140.01	3.62	0.66	0.02	0.68
24	7.38	140.38	25.13	0.68	0.02	0.70
25	7.38	216.62	24.38	1.58	0.02	1.59
26	7.38	222.62	24.38	7.37	0.02	7.38
27	7.38	262.03	23.16	7.71	0.02	7.73
28	35.45	258.95	23.16	36.89	0.09	36.98
29	5.38	438.29	22.00	6.76	0.01	6.77
30	5.38	224.35	4.10	4.41	0.01	4.43
31	8.47	204.25	4.10	6.79	0.02	6.81
32	8.47	146.37	4.32	6.46	0.02	6.49
33	0.32	146.37	4.32	0.24	0.00	0.24
34	8.78	140.01	3.62	0.79	0.02	0.81
35	8.78	140.02	4.32	0.79	0.02	0.81
36	8.78	146.37	4.32	6.71	0.02	6.73
37	28.07	140.01	3.62	2.52	0.07	2.59
38	28.07	141.80	134.56	2.93	0.07	3.00
39	20.07	325.17	130.53	9.76	0.05	9.81
40	20.07	331.17	130.53	22.04	0.05	22.09
41	28.07	488.66	124.00	41.05	0.07	41.12
42	28.07	258.14	23.16	29.18	0.07	29.25
43	13.85	212.03	4.10	11.20	0.04	11.24
44	13.85	32.88	0.05	1.76	0.04	1.80
45	43.91	32.88	0.05	0.09	0.11	0.20
46	10044.15	15.00	1.01	0.00	15.63	15.63
47	217.72	15.00	1.01	0.00	0.54	0.54
48	143.49	21.00	1.01	0.04	0.36	0.40
49	10118.39	18.15	1.01	0.51	14.47	14.98
50	5.38	258.95	23.16	5.60	0.01	5.62
51	30.07	258.95	23.16	31.29	0.08	31.36
52	30.07	32.88	0.05	3.71	0.08	3.78
53	43.91	32.88	0.05	5.47	0.11	5.58
54	20.07	141.80	134.56	2.09	0.05	2.14
55	8.00	141.80	134.56	0.84	0.02	0.86
56	8.00	325.00	130.53	3.89	0.02	3.91
57	8.00	329.36	127.53	8.80	0.02	8.82
58	8.00	629.55	124.00	13.61	0.02	13.63
59	20.07	438.29	124.00	27.57	0.05	27.62
60	14.00	562.83	49.80	19.35	721.47	740.82
61	69.55	1000.00	8.57	90.15	18.95	109.10
62	69.55	656.26	1.09	46.04	18.95	64.98
63	35.55	656.26	1.09	23.53	9.69	33.22
64	35.55	518.00	1.08	18.14	9.69	27.82
65	35.55	348.55	1.08	12.55	9.69	22.24
66	35.55	213.65	1.07	9.15	9.69	18.83
67	39.02	30.00	1.02	0.06	18.87	18.93
68	30.53	30.00	1.02	0.05	0.08	0.12
69	39.02	136.31	3.22	3.33	18.87	22.20
70	38.70	40.00	3.21	2.55	18.87	21.43
71	0.32	40.00	3.21	0.00	0.00	0.00
72	38.70	150.77	10.22	5.94	18.87	24.81
73	38.44	40.00	10.21	5.00	18.88	23.87
74	0.26	40.00	10.21	0.00	0.00	0.00

(*continued on next page*)

Table A.1 (*continued*)

Stream (j)	m_j (kg/s)	T_j (°C)	p_j (bar)	$\dot{E}_j^{PH}$ (MW)	$\dot{E}_j^{CH}$ (MW)	$\dot{E}_j^{tot}$ (MW)
75	38.44	150.77	32.46	8.32	18.88	27.20
76	38.36	40.00	32.45	7.44	18.89	26.33
77	0.08	40.00	32.45	0.00	0.00	0.00
78	38.36	151.73	103.09	10.76	18.89	29.66
79	38.33	30.00	103.09	9.87	18.90	28.77
80	0.03	30.00	103.09	0.00	0.00	0.00
81	282.26	458.29	1.06	53.49	1.97	55.45
82	159.15	1000.00	9.03	130.38	3.21	133.59
83	105.86	674.00	9.50	104.04	959.63	1063.67
84	91.86	1027.47	10.00	129.47	208.03	337.50
85	91.86	1000.00	9.03	124.72	208.03	332.75
86	153.38	1000.00	9.03	208.26	347.36	555.61
87	61.52	1000.00	9.03	83.53	139.33	222.86
88	34.00	565.26	1.09	22.50	9.26	31.77
89	34.00	205.02	1.04	8.49	9.26	17.75
90	69.55	209.43	1.04	17.55	18.95	36.49
91	206.67	303.85	9.50	57.33	0.32	57.65
92	131.15	303.85	9.50	36.38	0.20	36.59
93	206.67	424.47	9.50	71.85	0.32	72.17
94	290.29	698.85	9.03	159.27	1.44	160.71

and 92). Stream 91 is preheated in an air preheater (APH) by the gas exiting the main expander of the plant (GT1) and is fed to the cathode of the SOFC stacks (Stream 93). The oxygen contained in this stream is transported from the cathode to the anode of the cell through the electrolyte. Stream 92 is mixed with the oxygen-depleted air (Stream 82) exiting the cathode of the SOFC stacks and is fed to the cathode of the afterburner. The exhaust gas from the anode of the SOFC stacks, which contains H_2O, CO_2, as well as unused H_2 and CO, is fed into the AFB. The anode and cathode gases are kept separate in both the SOFC and the AFB.

The flue gas exiting the cathode of the AFB (Stream 4) is expanded in GT1. The gas then passes through the APH, enters the three-pressure-level heat-recovery steam generator (HRSG) and is exhausted to the environment (Stream 18). In the HRSG, steam is produced and expanded in the steam turbine (ST) of the plant. Part of the generated steam is fed to an additional steam turbine (ST4) that drives the hot gas fan (C6) and the CO_2 compressors (C2-C5).

The gas exiting the anode of the AFB (Stream 61) contains mainly water vapor and CO_2 and is expanded in the secondary gas turbine of the plant (GT2). After the expansion, the CO_2-rich gas is separated into two parts: one part is used to preheat the incoming fuel in a natural-gas preheater (NGPH) and the remainder is sent to the secondary HRSG of the plant (SH II, EV II, EC II). The CO_2 included in Stream 90 is isolated, while the included water is condensed in the four-stage, intercooled compression unit (C2-C5). Stream 79 contains approximately 99% CO_2 ready for transport and storage.

4. Results and discussion

The definitions of the exergetic efficiencies of selected plant components are presented in Table 2. Some cases require the separation of exergy into physical and chemical parts. For dissipative components, such as the particle filter, the absorber, and the inverter, the exergy of the product cannot be defined [37]. In Table 3, the exergy of incoming and outgoing/product streams is shown. The thermodynamic data at the stream level can be found in the Table A.1 of the paper.

The Grassmann diagram of the SOFC plant is shown in Fig. 3. The plant produces a net amount of electricity of 482 MW with an overall exergetic efficiency of 71%. Close to 60% of the total power output is generated in the fuel-cell stacks, 30% in the expanders of the plant (GT1 and GT2) and only 7% in the steam turbine. The results of the exergetic analysis for selected components and for the overall plant are shown in Table 4.

In general, the calculated exergetic efficiencies of the components of the SOFC plant are within expected value ranges [33]. High absolute values of exergy destruction are calculated for the SOFC stacks, the AFB, the PR, GT1, and C1. Although the PR, the SOFC and the AFB operate with relatively high exergetic efficiencies, they are responsible for approximately 54% of the overall exergy destruction, due to the high inefficiencies linked to the chemical reactions taking place there. Although specific measures can be taken to improve the efficiency of exothermic chemical reactors, such as preheating the incoming streams, it has been shown that most of the exergy destruction within such components is unavoidable [31,38,39]. It should also be mentioned that the efficiency of an SOFC is limited by its scale. One measure to achieve better performance of the examined SOFC unit would be to improve its voltage characteristics in order to decrease the exergy destruction of the electrochemical reaction. Other measures to improve the cost effectiveness of the considered plant could include the elimination of the steam turbine, because the power generated there is relatively low. This would also decrease the overall investment cost of the plant.

4.1. Comparison of the SOFC plant with the reference plant and alternative CO_2 capture plants

When comparing the individual results of common plant components of the SOFC and reference plants, we see that the efficiencies are comparable. However, we note a relatively large difference in the exergy of the fuel and product for the majority of the components. Specifically, large differences are found for the GT and ST systems of plants, which in the SOFC plant operate with significantly smaller mass flow rates. Although smaller mass flow rates result in the use of smaller components, they also result in a decrease of the available thermal energy in the flue gases and, thus, reduce the production of steam in the Rankine cycle of the SOFC plant.

Nevertheless, when looking at the overall plants, the results favor the SOFC plant. Although the reference plant receives the same amount of fuel as the SOFC plant, it produces 412 MW with an exergetic efficiency of 56.1%. Thus, compared to the SOFC plant, the reference plant performs with a substantially lower efficiency that results in a significantly lower power output. Although electricity is required to compress the separated CO_2 in the SOFC plant, the overall power generation of the plant, which consists of

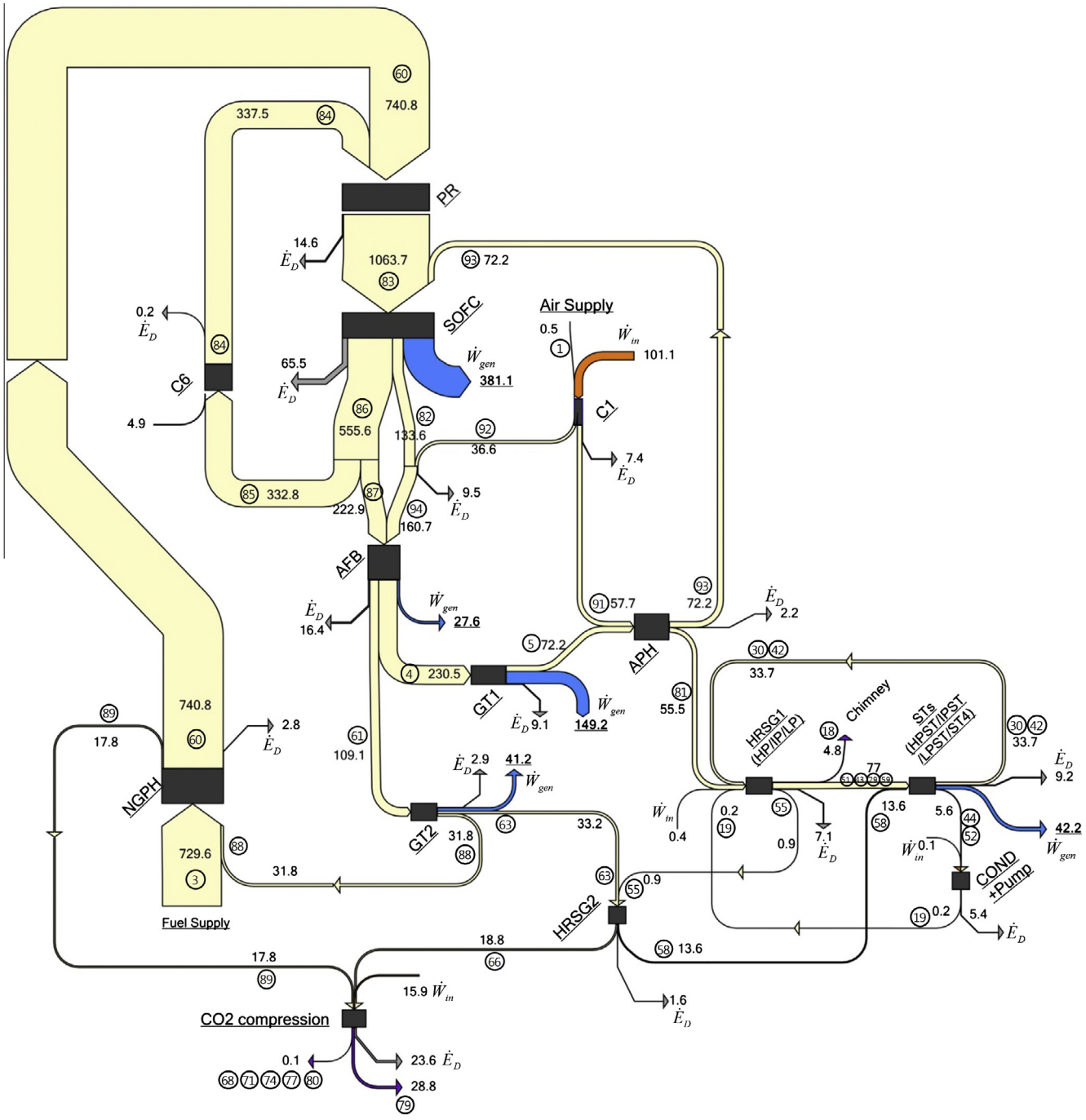

Fig. 3. Grassmann diagram of the SOFC plant.

the power generated in the gas turbines, the steam turbines, the SOFC and the AFB, significantly surpasses that of the reference plant.

Other CO_2 capture alternatives incorporated into the reference plant and simulated under similar conditions are presented in [40,41]. The most efficient technologies among the alternatives examined in ref. [29] were two oxy-fuel power plants. The first one included chemical looping combustion (CLC plant) and the second one a mixed conducting membrane reactor (AZEP concept). When comparing the SOFC plant with these plants, we again find significant differences in component sizes. Since the component sizes of the AZEP and CLC plants agreed in general with those of the reference plant, the plants included streams of similar mass flow rates [29]. Nevertheless, since the amount of the fuel and, thus, the amount of the generated CO_2 emissions is the same in all considered power plants, the results of the CO_2 compression unit is similar in all concepts including CO_2 capture.

The essential difference between the SOFC plant and the other capture alternatives lies in the resulting efficiency. While the AZEP and CLC plants operate with a lower efficiency than the reference plant, the SOFC plant has a higher efficiency because of the electricity produced in its SOFC and AFB. In this way, the SOFC plant is found to be thermodynamically superior when compared with the other alternatives. It should be mentioned, however, that the expected cost of electricity (COE) generated from the SOFC plant would likely be significantly higher than the COE from the other concepts.

Table 4
Results for selected plant components of the SOFC plant.

Component k	$\dot{E}_{F,k}$ (MW)	$\dot{E}_{P,k}$ (MW)	$\dot{E}_{D,k}$ (MW)	$y_{D,k}$ (%)	ε_k (%)
C1	101.1	93.7	7.42	4.18	92.7
GT1	158.3	149.2	9.08	5.11	94.3
PR	44.8	30.1	14.64	8.24	67.3
SOFC	609.4	543.9	65.51	36.89	89.3
AFB	119.9	103.5	16.39	9.23	86.3
GT2	44.1	41.2	2.90	1.64	93.4
HPST	11.9	11.0	0.85	0.48	92.8
IPST	2.3	2.2	0.15	0.09	93.6
LPST	9.4	8.2	1.28	0.72	86.4
ST4	27.6	20.8	6.74	3.79	75.6
APH	16.7	14.5	2.22	1.25	86.7
NGPH	14.0	11.2	2.82	1.59	79.9
RH	1.4	1.2	0.24	0.14	82.6
HPSH	6.1	5.5	0.53	0.30	91.3
HPEV	13.2	12.3	0.96	0.54	92.7
HPEC	9.1	7.7	1.47	0.83	83.9
IPSH	0.4	0.3	0.08	0.05	80.6
IPEV	6.3	5.8	0.56	0.31	91.2
IPEC	1.1	0.9	0.17	0.10	84.0
LPSH	0.5	0.3	0.13	0.07	71.6
LPEV	7.2	5.9	1.27	0.71	82.3
LPEC	5.3	3.6	1.68	0.95	68.3
SH II	5.4	4.8	0.58	0.33	89.2
EV II	5.6	4.9	0.67	0.38	88.0
EC II	3.4	3.1	0.35	0.20	89.6
C2	3.9	3.3	0.62	0.35	84.1
C3	4.0	3.4	0.65	0.37	83.8
C4	4.0	3.3	0.65	0.37	83.6
C5	4.0	3.3	0.68	0.38	83.0
C6/Fan	4.9	4.7	0.19	0.10	96.2
Total	730.2	518.9	177.58	100.00	71.1

In general, CO_2 capture is energy intensive and the main disadvantage of most technologies is that they significantly decrease the operational efficiencies of the plants. The oxy-fuel plants discussed here are relatively efficient because they perform the oxygen separation without the use of an air separation unit, which consumes significant amounts of energy. However, they are still associated with significant efficiency penalties when compared to business as usual scenarios. SOFC plants can overcome this problem by generating additional power that makes up for the energy needs of the CO_2 compression unit. Nevertheless, to achieve further progression for large-scale SOFC plants, the implementation challenges of SOFC units must be resolved, while the economic and environmental performance of SOFC plants must be considered as well.

5. Conclusions

In this paper, an exergetic analysis was used to evaluate a combined-cycle power plant including a solid-oxide fuel cell and CO_2 capture and compression. The plant was simulated using data from a conventional reference plant without CO_2 capture and was compared both with the reference plant and with other plants with alternative capture technologies.

The fuel-cell stacks, afterburner and expanders cause most of the exergy destruction within the solid-oxide fuel cell plant. Although inefficiencies related to chemical reactions are mostly unavoidable, improvements could be achieved by eliminating sub-processes that increase the exergy destruction or the exergy loss, and burden the capital investment of the structure. The overall exergetic efficiency of the fuel-cell plant (71.1%) was found to be significantly higher than that of the reference plant (56.5%), due to the additional power produced in the fuel-cell stacks and afterburner of the plant. In addition, the thermodynamic efficiency of the examined power plant seems promising, especially when compared to other alternatives for CO_2 capture.

Acknowledgements

Dr. Fontina Petrakopoulou would like to thank the IEF Marie Curie Action PEOPLE-2012-IEF-GENERGIS-332028 funded by FP7.

References

[1] Fuel Cell Today. The Fuel Cell Today Industry, Review. 2011.
[2] NETL. Fuel Cell Handbook. University Press of the Pacific; 2005.
[3] Harvey SP, Richter HJ. Improved gas turbine power plant efficiency by use of recycled exhaust gases and fuel cell technology. Advanced Energy Systems Division (AES), 1993, p. 199–207.
[4] Lundberg WL, Lsraelson GA, Moritz RR, Veyo SE, Holmes RA, Zafred PR, et al. Pressurized Solid Oxide Fuel Cell/ Gas Turbine Power, System. 2000.
[5] Chan S. Multi-level modeling of SOFC–gas turbine hybrid system. International Journal of Hydrogen Energy 2003;28:889–900.
[6] Kuchonthara P, Bhattacharya S, Tsutsumi A. Combinations of solid oxide fuel cell and several enhanced gas turbine cycles. Journal of Power Sources 2003;124:65–75.
[7] Kabata T, Nishiura M, Tomida K, Koga S, Matake N, Ando Y, et al. Development of the 200kW Class SOFC-MGT Combined Cycle System with Tubular Type Cell Stack. Fuel Cell Seminar & Exposition, 2008, p. 263–7.
[8] Calise F, Palombo A, Vanoli L. Design and partial load exergy analysis of hybrid SOFC–GT power plant. Journal of Power Sources 2006;158:225–44.
[9] Onda K, Iwanari T, Miyauchi N, Ito K, Ohba T, Sakaki Y, et al. Cycle Analysis of Combined Power Generation by Planar SOFC and Gas Turbine Considering Cell Temperature and Current Density Distributions. Journal of The Electrochemical Society 2003;150:A1569–76.
[10] Rao AD, Samuelsen GS. A Thermodynamic Analysis of Tubular SOFC based Hybrid Systems. ASME Journal of Gas Turbines and Power 2003;125:59–66.
[11] Panopoulos KD, Fryda LE, Karl J, Poulou S, Kakaras E. High temperature solid oxide fuel cell integrated with novel allothermal biomass gasification. Journal of Power Sources 2006;159:570–85.
[12] El-Emam RS, Dincer I, Naterer GF. Energy and exergy analyses of an integrated SOFC and coal gasification system. International Journal of Hydrogen Energy 2012;37:1689–97.
[13] Akkaya A, Sahin B, Huseyinerdem H. An analysis of SOFC/GT CHP system based on exergetic performance criteria. International Journal of Hydrogen Energy 2008;33:2566–77.
[14] Zink F, Lu Y, Schaefer L. A solid oxide fuel cell system for buildings. Energy Conversion and Management 2007;48:809–18.

[15] Gadalla M, Al Aid N. Thermodynamic Modeling and Energy Analysis of a SOFC-PEMFC Combination in a Gas Turbine Cycle. 8th International Fuel Cell Science, Engineering and Technology Conference: Volume 2, vol. 2010, ASME; 2010, p. 283–94.
[16] Al-Sulaiman FA, Dincer I, Hamdullahpur F. Energy analysis of a trigeneration plant based on solid oxide fuel cell and organic Rankine cycle. International Journal of Hydrogen Energy 2010;35:5104–13.
[17] Rajashekara K. Hybrid Fuel-Cell Strategies for Clean Power Generation. IEEE Transactions on Industry Applications 2005;41:682–9.
[18] De Guire EJ. Solid Oxide Fuel Cells, Review Article 2003.
[19] Duan L, Zhang X, Yang Y. Exergy analysis of a novel SOFC hybrid system with zero CO2 emission. In: Benini E, editor. Advances in Gas Turbine Technology, InTech; 2011, p. 19.
[20] IPCC Special Report - Carbon Dioxide Capture and Storage — Working Group III. Cambridge, United Kingdom and New York, NY, USA: Cambridge University Press; 2005.
[21] Ou X, Xiaoyu Y, Zhang X. Life-cycle energy consumption and greenhouse gas emissions for electricity generation and supply in China. Applied Energy 2011;88:289–97.
[22] Li H, Yan J, Anheden M. Impurity impacts on the purification process in oxy-fuel combustion based CO_2 capture and storage system. Applied Energy 2009;86:202–13.
[23] Chen S, Xiang W, Wang D, Xue Z. Incorporating IGCC and CaO sorption-enhanced process for power generation with CO_2 capture. Applied Energy 2012;95:285–94.
[24] Park SK, Kim TS, Sohn JL, Lee YD. An integrated power generation system combining solid oxide fuel cell and oxy-fuel combustion for high performance and CO_2 capture. Applied Energy 2011;88:1187–96.
[25] Li M, Rao AD. Scott Samuelsen G. Performance and costs of advanced sustainable central power plants with CCS and H_2 co-production. Applied Energy 2012;91:43–50.
[26] Kvamsdal HM, Jordal K, Bolland O. A quantitative comparison of gas turbine cycles with CO_2 capture. Energy 2007;32:10–24.
[27] Maurstad O, Bredesen R, Bolland O, Kvamsdal H, Schell M. SOFC and gas turbine power systems - evaluation of configurations for CO_2 capture. GHGT-7, Vancouver: 2004.
[28] Haines MR, Heidug WK, Li KJ, Moore JB. Progress with the development of a CO_2 capturing solid oxide fuel cell. Journal of Power Sources 2002;106:377–80.
[29] Petrakopoulou F. Comparative Evaluation of Power Plants with CO_2 Capture: Thermodynamic, Economic and Environmental Performance. Ph.D. Thesis, Technische Universität Berlin, 2010.
[30] Petrakopoulou F, Boyano A, Cabrera M, Tsatsaronis G. Exergoeconomic and exergoenvironmental analyses of a combined cycle power plant with chemical looping technology. International Journal of Greenhouse Gas Control 2011;5:475–82.
[31] Petrakopoulou F, Tsatsaronis G, Morosuk T, Carassai A. Conventional and advanced exergetic analyses applied to a combined cycle power plant. Energy 2012;41:146–52.
[32] Petrakopoulou F, Tsatsaronis G, Boyano A, Morosuk T. Exergoeconomic and exergoenvironmental evaluation of power plants including CO_2 capture. Chemical Engineering Research and Design 2011;89:1461–9.
[33] Bejan A, Tsatsaronis G, Moran M. Thermal Design and Optimization. New York: Wiley-Interscience; 1996.
[34] Tsatsaronis G, Cziesla F. Thermoeconomics. Encyclopedia of Physical Science and Technology, Academic Press; 2002, p. 659–80.
[35] SteagEnergyServices. EBSILONProfessional 2012.
[36] Riensche E, Meusinger J, Stimming U, Unverzagt G. Optimization of a 200 kW SOFC cogeneration power plant. Part II: variation of the flowsheet. Journal of Power Sources 1998;71:306–14.
[37] Tsatsaronis G. Cziesla F. Encyclopedia of Life Support System (EOLSS): Energetic and exergetic analysis of complex systems; 2004.
[38] Petrakopoulou F, Tsatsaronis G, Morosuk T. CO_2 capture in a chemical looping combustion power plant evaluated with an advanced exergetic analysis. Environmental Progress & Sustainable Energy 2013, http://dx.doi.org/10.1002/ep.11848.
[39] Morosuk T, Tsatsaronis G. How to Calculate the Parts of Exergy Destruction in an Advanced Exergetic Analysis. In: Ziebik A, Kolenda Z, Stanek W, editors. Proceedings of the 21st International Conference on Efficiency. Optimization, Simulation and Environmental Impact of Energy Systems, Cracow, Gliwice: Costs; 2008. p. 185–94.
[40] Petrakopoulou F, Tsatsaronis G, Morosuk T. Conventional Exergetic and Exergoeconomic Analyses of a Power Plant with Chemical Looping Combustion for CO_2 Capture. International Journal of Thermodynamics 2010;13:77–86.
[41] Petrakopoulou F, Tsatsaronis G, Morosuk T. Exergoeconomic Analysis of an Advanced Zero Emission Plant. ASME Journal of Engineering for Gas Turbines and Power 2011;133:113001–12.